

Facile Electrical DNA Genosensor for Human Papillomavirus (HPV 58) for Early Detection of Cervical Cancer

F. Nadhirah Jaapar¹, N. A. Parmin^{1*}, N. Hamidah A Halim¹, Uda Hashim¹, Subash C.B. Gopinath¹, A. Rahim Ruslinda¹, Sh. Nadzirah², C.H. Voon¹, M.N.A. Uda¹, Wei Chern Ang³, Iffah Izzati Zakaria⁴, Zulida Rejali⁵, Amilia Afzan⁵, Azrul Azlan Hamzah², Chang Fu Dee², F. Syakirah Halim¹

¹Institute of Nano Electronic Engineering, Universiti Malaysia Perlis, 01000 Kangar, Perlis, Malaysia;

²Institute of Microengineering and Nanoelectronics, Universiti Kebangsaan Malaysia, 43600 Bangi, Selangor, Malaysia;

³Clinical Research Centre, Ministry of Health Malaysia, Hospital Tuanku Fauziah, 01000 Kangar, Perlis, Malaysia;

⁴Malaysia Genome Institute, Jalan Bangi, 43000, Kajang, Selangor;

⁵Department of Obstetrics and Gynaecology (O&G), Faculty of Medicine & Health Sciences, Universiti Putra Malaysia, 43400 UPM Serdang, Selangor.

Received 18 July 2022, Revised 25 July 2022, Accepted 10 August 2023

ABSTRACT

For decades, a Pap smear test has been applied as a conventional method in detecting Human Papillomavirus caused cervical cancer. False-positive results were also recorded while using it as conventional method. Current biosensor such as Hybrid (II) Capture resulted in higher time consumption and cost. Meanwhile, in this study we provided facile, mini, rapid, highly sensitive, eco-friendly, and cost-effective sensing system focusing on HPV strain 58 (HPV58) in a nano-size lab-on-chip technology genosensor. 30-mer of virus ssDNA designed and analyzed as a probe via bioinformatics tools such as GenBank, Basic Local Alignment Searching Tools (BLAST) and ClustalW. Nanotechnology-developed colloidal Gold-nanoparticles (AuNPs) are used in the biosensor fabrication to produce high stability and electron efficient transmission during electrical measurement. AuNPs-APTES modified on active sites of IDEs, followed by immobilization of specific probe ssDNA for HPV 58. Hydrogen binding during hybridization with its target produce electrical signals measured by KEITHLEY 2450 (Source Meter). The genosensor validated with different types of targets such as complimentary, non-complementary and single mismatch oligonucleotides. The serial dilution of target concentration has been experimented triplicate (n=3) range from 1fM to 10µM. The slope of calibration curve resulted 2.389E-0 AM⁻¹ with regression coefficient (R²) = 0.97535.

Keywords: Bioinformatics tools, cervical cancer, DNA genosensor, gold-nanoparticles, Human Papillomavirus

1. INTRODUCTION

Cervical cancer is a world's third leading cancer-related mortalities as more than 200 000 death recorded from 1985 until 2020 [1]. Most of the reasons are due to the lack of awareness and control

* Corresponding author: azizahparmin@unimap.edu.my

measures applied. For the past few years, *Papanicolaou* Test or Pap Smear test has been used to screen and analyze abnormal cells detected on the cervix [2]. Precancerous cells were scraped and brushed from the cervix then examined in the lab for abnormalities. This procedure also implicated colposcopy procedure. Regarding the hardship of the process, it resulted from flying in the ointment, such as increased risks of giving birth and the accuracy of the test may lower (false positive and false negative results) [3].

Human Papillomavirus (HPV) is a virus causing cervical cancer during sexual interaction. On the other hand, the virus was transferred primarily by skin-to-skin contact due to contagious warts. HPV is a virus that can cause cervical cancer that can only be detected after squamous cell carcinoma or adenocarcinoma is invaded into a malignant cell on the cervix. HPV-58 is categorized as Alpha-papillomavirus (high-risk) as it spreads on mucosal lesion of cervix similar with HPV 16 and HPV 18 [4]–[6]. In addition, 85% of cervical cancer is caused by Alpha-papillomavirus as it is listed as the most oncogenic HPV. Meanwhile, there were HPV strains listed as low risk HPV such as HPV 6 and HPV 11 which produce non genital warts that are not transmitted sexually [7].

Interdigitated Electrodes (IDE) with 10 nm of finger gaps works as a substrate film in this study to analyze the current behaviors of biochemical reaction of HPV and AuNPs during hybridization process. This is an electrical analysis method on DNA probe bind with the specific target of HPV 58. The analysis usually conveyed dipole moment stated as sensitivity and selective of the DNA probe and the target. The method is also regarded as an electrical analysis system for early detection of cervical cancer. Most of the time, the data analysis graphically shown as I-V analysis using picoammeter up to 1 V voltage source.

In this study, IDEs were designed by AutoCAD and fabricated by Silterra coated with silicone dioxide. On the top of silicone dioxide, smaller finger gaps of titanium oxide layered to increase the surface volume to ratio during detection DNA probe with its target [8], [9]. IDEs based electrical genosensor can be used for label-free and facile on early detection of cervical cancer.

Gold-nanoparticles (AuNPs) in colloidal particles applied for surface modification on the IDEs before immobilization of DNA probe and target. In addition, colloidal AuNPs are synthesized with citrate buffer which helps to stabilize and prevent them from accumulating. The layer on the surface of nanoparticles formed via citrate ions which keeps them separated and prevents from clumping together. The details of AuNPs also outline the higher affinity binding with silicone substrates and super corrosion resistance [10]–[12]. According to previous research, modification of active area with AuNPs have wider potential on detecting high-risk HPV at early stage as it consists of abundance hydroxyl group and more stable [13]–[15]. The scientific justification proved the biosensor successfully identified the HPV extracted from the real samples aided with AuNPs as electron catalyst during electrochemical analysis [16]. Hence, it can be gold standard for this study as Mahmoodi *et al* also aimed on early detection of high-risk HPV (HPV 18)[16].

The major steps in this study are, surface modification of colloidal AuNPs, silanization process by (3-Aminopropyl) triethoxysilane (APTES), immobilization of DNA probe and hybridization of probe with its target from HPV 58. To the best of our knowledge, this study enlightens the method of analysis on early detection of HPV 58 by electrical-based IDEs with surface modification of colloidal AuNPs.

2. MATERIALS AND METHOD

2.1 Chemical, reagents, and instruments

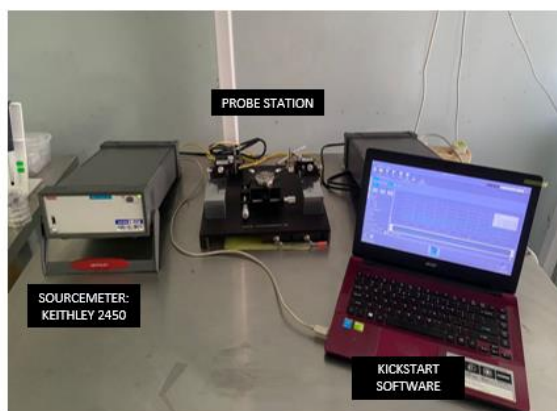
The chemical solution such as colloidal AuNPs, Gold chloride trihydrate ($\text{HAuCl}_4 \cdot 3\text{H}_2\text{O}$) (10nm), (3-Aminopropyl) triethoxysilane (APTES), Deionized water (DI Water) and Diethylpyrocarbonate (DEPC) treated water were obtained from Sigma Aldrich and Thermo-Scientific (USA). Meanwhile, biological solution such as 30-mer sequence of synthetic DNA probe and target for HPV 58 obtained from Biotek Abadi Sdn Bhd (MY). DI water focused on serial dilution involving chemical solution while DEPC water for biological solution as it is nuclease-free.

2.2 Designation DNA probe

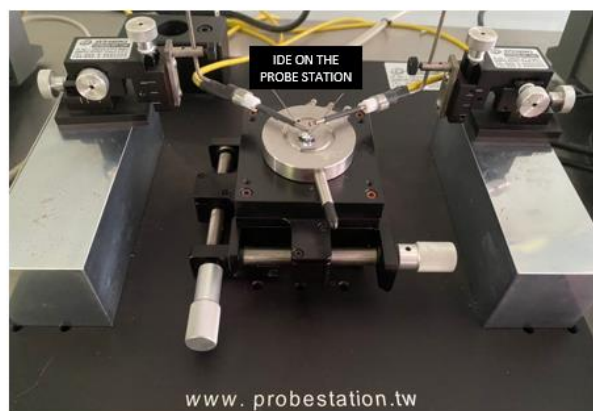
DNA probe for HPV 58 designed from E6 region from whole genome. The region highlighted higher protuberant probability annealing than consensus probe and helps in strengthening the decimation of various core administrative protein of host genome [17]. 30-mer DNA sequence designed by bioinformatics tools; GenBank (<https://www.ncbi.nlm.nih.gov/genbank/>) and the similarities finalized by Basic Local Alignment Searching Tools (BLAST) (<https://blast.ncbi.nlm.nih.gov/Blast.cgi>). To enhance its efficiency, CLUSTAL OMEGA served multiple sequence alignment with different HPV strains whole genome. The output of BLAST must in 100% similarities compared with same HPV strains in the database.

2.3 Electrical characterization on IDE

The completed IDEs devices were inspected using Source Meter, KEITHLEY 2450 to observe its current behaviors under 1V source of voltage. As it is produced in bulk, some IDEs may experience current shortage preventing the detection of HPV 58. By using KEITHLEY 2450, the software package included is KickStart and the voltage was prescribed from 0V to 1 V. A probe station is interconnected between KEITHLEY 2450 and KickStart software as shown in Figure 1. During the electrical measurement, the IDE placed on the probe station connected with source of voltage and the output shown in the KickStart software also shown in Figure 1.



A)



B)

Figure 1. Electrical characterization. A) Setup for electrical characterization with Source Meter (KEITHLEY 2450) and software (KickStart); B) Position of the IDE on the probe station connected with source of voltage.

2.4 Surface modification on IDE via colloidal AuNPs

Before surface modification by colloidal AuNPs, piranha cleaning is conducted on each IDE before electrical characterization by Source Meter. By focusing on silicon wafer, mixture of 3mL of hydrogen peroxide with 6mL of sulfuric acid (1:3) applied to remove any organic matter preventing contamination. Then, electrical characterization was applied to prevent any shortage of current during the experiment. After incubating for 30 minutes in room temperature, 2 μ L of colloidal AuNPs dropped cast on the active area of the IDEs continued with electrical measurement.

2.5 Silanization, Immobilization and Hybridization process

After surface modification, the IDEs with colloidal AuNPs undergo silanization process by APTES. The aim of silanization process is to construct hydrogen and covalent bonding between AuNPs and APTES by hydrolysis and dehydration synthesis process(Si-O-Au) [18]. During silanization process, 2 μ L of 12% APTES dropped cast on the same active site of colloidal AuNPs and incubated for 30 minutes in dry cabinet to form self-assembled monolayer. Then, IDE rinsed with DI water and incubated for 10 minutes. Next, the immobilization process created amide bond from carboxylic acid (COOH) by DNA probe with amine group (NH₂) by APTES. 2 μ L of DNA probe dropped cast on the same active site and incubated for 15 minutes and rinsed with DEPC water to remove unbounded DNA probe. Blocking buffer such as polyethylene glycol (PEG) dropped on the same active area and incubated for 10 minutes. After 10 minutes, DI water is applied to rinse and incubate for 5 minutes. Hydrogen bonding is expected to form during hybridization process of DNA probe and its target. In this study, synthetic complementary, non-complementary and single mismatching strands were experimented for early detection of cervical cancer by HPV 58. In addition, different concentration of complementary strands also conducted range from 1fM to 10 μ M to observe the transition of current values. Figure 2 shows preparation steps on developing a facile DNA genosensor for HPV 58 for early detection of cervical cancer including silanization, immobilization and hybridization. Figure 2 shows the fundamentals of the study started with (A) piranha cleaning, (B) surface modification, (C) silanization, (D) immobilization and (E) hybridization process.

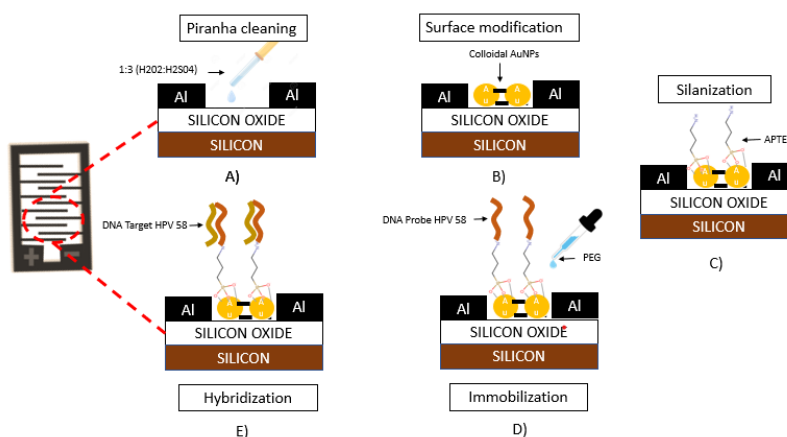


Figure 2. Fundamental of the study. A) Piranha cleaning, B) Surface modification by colloidal AuNPs, C) Silanization by APTES, D) Immobilization of DNA probe, E) Hybridization of complementary, non-complementary and single-mismatching strands.

3. RESULTS AND DISCUSSION

3.1 Designation of DNA probe from E6 region of HPV 58

DNA probes, complementary, non-complementary and single-mismatching strands have been designed with 30-mer length of nucleotides. The aim of designation multiple strands of target DNA is to observe the current behavior during hybridization process by electrical measurement. Table 1 shows 30-mer of nucleotides for DNA probe, complementary, non-complementary and single-mismatch strands from HPV 58. The 'red' base-pair changes in complementary and single mismatch indicated single alternation affected the hybridization process.

Table 1 30-mer of nucleotides for DNA probe strand, complementary strand, non-complementary and single mismatch

Type of ssDNA (HPV58)	Oligonucleotides
Probe	5'CGG GCC AGA TGG ACA AGC ACA ACC GGC CAC3'
Complementary	5' GTG GCC GGT TGT GCT TGT CCA TCT GGC CCG3'
Non-complementary	5'CAC CGG CCA ACA CGA ACA GGT AGA CCG GGC3'
Single mismatch	5' GTG GCC GGT TGT GCT TAT CCA TCT GGC CCG3'

3.2 Surface modification on IDEs

In Figure 3, IDEs have been analyzed and observed by using High Performance Microscope (HPM) with x50 magnification. In A), IDEs have been treated with piranha cleaning to remove impurities before colloidal AuNPs dropped cast on the active area. The surface topography of IDE shows uniform structure without any shortage of current and clean without impurities. Meanwhile, B) has shown the self-assemble monolayer of colloidal AuNPs on the active site of IDEs after depositing colloidal AuNPs. On the other hand, electrical measurement has been applied on bare IDEs and IDEs deposited with colloidal AuNPs. The analysis was to ensure and prove the electron transmission of colloidal AuNPs during electrical measurement. In this research, the electrical measurement of each sample was repeated triplicate (n=3) from 0V to 1V measured by Source Meter. As shown in Figure 4, current measurements for both IDE were gradually increased from 0V to 1V. On the other hand, the current measurement of IDEs deposited with AuNPs indicates at $8.1701\text{E}-10$ A is higher than $1.25112\text{E}-10$ A of bare IDEs at 1V. The phenomenon due to the hydrophilization reaction between the mixture of H_2SO_4 and H_2O_2 with colloidal AuNPs [19]. During the hydrophilization process, the hydroxyl group (OH) existed on the active site of IDEs and acted as electron linkage to enhance the conductivity of surface modification and performed a self-assembly monolayer on the first layer [20]. Self-assemble monolayer of AuNPs is fundamental of this study to strengthen the attachment of biological reaction and its biocompatibility. Thus, the current measurement of IDEs deposited with AuNP was recorded higher than bare IDEs. The effect of AuNPs deposited on the sensing area gives good agreement as AuNPs proved to be an electrical enhancer on the transducer. The surface modification of IDEs continued with the silanization process, which implemented relevant silane coupling agents with a higher tendency to form a permanent linkage between AuNPs and IDEs, preventing aggregations.

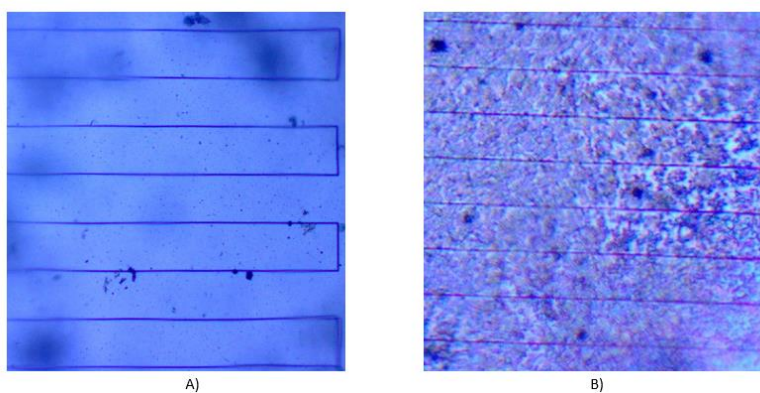


Figure 3. Surface topography of IDEs by HPM; A) Surface modification of IDEs before colloidal AuNPs deposited; B) Surface modification after colloidal AuNPs deposited.

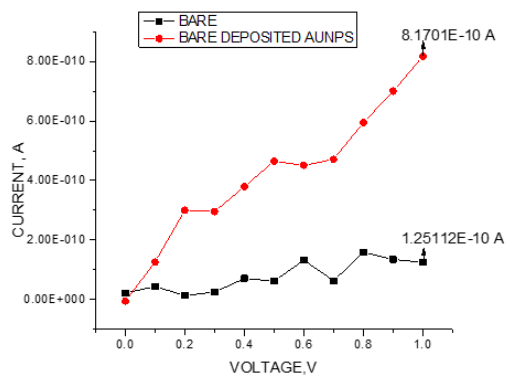


Figure 4. Electrical characterization on bare IDEs and IDEs deposited with AuNPs after surface modification analysis (n=3)

3.3 Electrical characterization of HPV 58 for cervical cancer detection

Electrical measurement of IDE started with a bare IDE after piranha cleaning. In this study, I-V measurement was conducted after each fundamental step started with surface modification, silanization, immobilization and hybridization process. The current measured on bare IDE was $2.505\text{E-}10$ A slightly lower than surface modification process by colloidal AuNPs which measured on $4.362\text{E-}10$ A. Higher measurement of current for surface modification by colloidal AuNPs proved they were higher in electron transmission [21]. The silanization process recorded $1.220\text{E-}8$ A current measurement of APTES resulted higher than surface modification process. This due to the hydrogen bonding during hydrolysis and dehydration synthesis between active site on bare IDE and APTES [22], [23]. The current measurement spiked after ssDNA probe immobilized on the same active sites and resulted $2.348\text{E-}07$ A which highest among the others.

The spike of current measured is due to the covalent bonding between amine group (NH_2) from APTES and carboxylic acid (COOH) forming amide bond [24], [25]. It is also due to the surface charge density from the negatively charged ssDNA phosphate backbone. On the contrary, current measurement on hybridization process resulted slightly lower than immobilization process recorded at $1.016\text{E-}07$ A. The declination of current measurement is due to abundance of negative charge which led to resistance during hybridization [8], [13], [17]. The process of hybridization with complementary target for HPV depicted in Figure 5. In addition, all current measurements were measured at maximum 1V.

Other than that, Figure 5 illustrates the current measurement for non-complementary and single mismatch target strands for selectivity test. The objective of the selective test was to study the probability of ssDNA probe to hybridize with other strands compared with complementary strands. As shown in Figure 5, the current measurements for complementary, non-complementary and single mismatch strands were gradually increased. However, hybridization process occurred only for complementary strand as only its current measurement was slightly lower than ssDNA probe. Meanwhile, the non-complementary strand recorded lower current measured on $4.146\text{E-}09$ A while single-mismatch was on $3.052\text{E-}08$ A at 1V compared with complementary strands. The lowest current recorded by non-complementary strand was because of non-hybridized oligonucleotides and led to obstruction of electron transmission.

The electrical test in Figure 5 was conducted at the same period to observe the similarity or discrepancy of each strand. Triplicate determinations of three independent repeated experiments have been experimented for both analyses. Thus, the experimental analyses in Figure 5 proved the selectivity and specificity of designed ssDNA probe which only can hybridize with complementary strand. The calibration curve of serial dilution of target concentration is illustrated clearly in Figure 5, which indicates the sensitivity of the DNA genosensor. The serial dilution of target concentration has been experimented triplicate ($n=3$) range from 1fM to $10\mu\text{M}$. As shown in Figure 5, the slope of the calibration curve is $2.389\text{E-}0$ AM^{-1} with regression coefficient (R^2) = 0.97535. Hence, the developed electrical based genosensor has wide potential in nanobiotechnology engineering as it can detect to the smallest concentration of the virus (1fM).

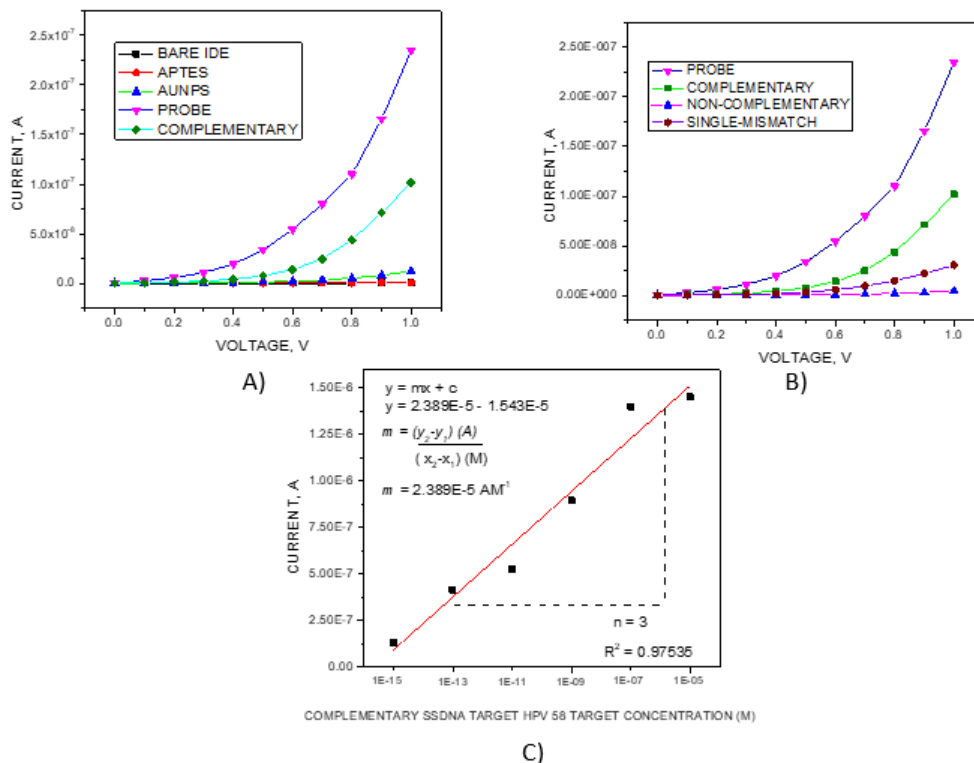


Figure 5. Electrical results via KEITHLEY 2450: A) Electrical test on complementary strands (HPV 58), B) Selectivity test by complementary, non-complementary and single mismatch strands (HPV 58), C) Sensitivity test on serial dilution of complementary strands ranged from 1fM to 10µM.

4. CONCLUSION

In this research, we described an approach on developing facile DNA genosensor for early detection of cervical cancer by HPV 58 strain. Our DNA genosensor proved its efficiency as it can directly detect current from small range until large range on serial concentration of ssDNA target. The self-assemble monolayer of colloidal AuNPs demonstrated higher current compared with bare IDE led to the higher electron transmission during surface modification process. The surface modification via colloidal AuNPs also proves its biocompatibility and stability ensuring its reliability for early detection of HPV for cervical cancer. According to calibration curve results, the sensitivity of genosensor can be proved with the regression coefficient up to 97%. Meanwhile, the selectivity of this DNA genosensor is beyond doubt as it can identify the non-complementary and single mismatch target strands and illustrated on current measurement. Thus, we hope this fundamental can be applied as an evolutionary method replacing conventional methods such as Pap Smear test in the future.

ACKNOWLEDGEMENTS

The author would like to thank all staff members of the Institute of Nano-electronic Engineering in Universiti Malaysia Perlis (UniMAP) for their technical advice and contributions, directly and indirectly. This research was supported by the Ministry of Higher Education (MOHE) under Grant no. RACER/ 1/2019/TK04/UNIMAP//2.

REFERENCES

- [1] M. Kasraeian *et al.*, "Patients' self-reported factors influencing cervical cancer screening uptake among HIV-positive women in low- and middle-income countries: An integrative review," *Gynecol. Oncol. Reports*, vol. 33, no. March, p. 100596, 2020, doi: 10.1016/j.gore.2020.100596.
- [2] L. Xu, Q. Xu, X. Li, and X. Zhang, "MicroRNA-21 regulates the proliferation and apoptosis of cervical cancer cells via tumor necrosis factor- α ," *Mol. Med. Rep.*, vol. 16, no. 4, pp. 4659–4663, 2017, doi: 10.3892/mmr.2017.7143.
- [3] W. P. S. Ezat, "Cost-effectiveness of HPV vaccination against cervical cancer in Malaysia," *Asian Pacific J. Cancer Prev.*, vol. 11, pp. 79–90, 2010.
- [4] R. Ghittoni, R. Accardi, S. Chiocca, and M. Tommasino, "Role of human papillomaviruses in carcinogenesis," *Ecancermedicalscience*, vol. 9, pp. 1–9, 2015, doi: 10.3332/ecancer.2015.526.
- [5] R. D. Burk, A. Harari, and Z. Chen, "Human papillomavirus genome variants," *Virology*, vol. 445, no. 1–2, pp. 232–243, 2013, doi: 10.1016/j.virol.2013.07.018.
- [6] J. Fernandes, "Biology and natural history of human papillomavirus infection," *Open Access J. ...*, vol. 5, pp. 1–12, 2013, doi: 10.2147/OAJCT.S37741.
- [7] A. S. Amrul Muhadi *et al.*, "Gold Nanoparticles Enhanced Electrochemical Impedance Sensor (EIS) for Human Papillomavirus (HPV) 16 Detection E6 region," *IOP Conf. Ser. Mater. Sci. Eng.*, vol. 864, no. 1, 2020, doi: 10.1088/1757-899X/864/1/012165.
- [8] N. A. Parmin *et al.*, "Voltammetric determination of human papillomavirus 16 DNA by using interdigitated electrodes modified with titanium dioxide nanoparticles," *Microchim. Acta*, vol. 186, no. 6, 2019, doi: 10.1007/s00604-019-3445-2.
- [9] N. A. Parmin, U. Hashim, N. Hamidah A Halim, M. N. A. Uda, and M. N. Afnan Uda, "Characterization of Genome Sequence 2019 Novel Coronavirus (2019-nCoV) by using BioinformaticTool," *IOP Conf. Ser. Mater. Sci. Eng.*, vol. 864, no. 1, 2020, doi: 10.1088/1757-899X/864/1/012168.
- [10] K. Y. P. S. Avelino, L. S. Oliveira, N. Lucena-Silva, C. P. de Melo, C. A. S. Andrade, and M. D. L. Oliveira, "Metal-polymer hybrid nanomaterial for impedimetric detection of human papillomavirus in cervical specimens," *J. Pharm. Biomed. Anal.*, vol. 185, 2020, doi: 10.1016/j.jpba.2020.113249.
- [11] B. Karlik, M. F. Yilmaz, M. Ozdemir, C. T. Yavuz, and Y. Danisman, "A Hybrid Machine Learning Model to Study UV-Vis Spectra of Gold Nanospheres," *Plasmonics*, vol. 16, no. 1, pp. 147–155, 2021, doi: 10.1007/s11468-020-01267-8.
- [12] J. H. Lee, H. Y. Cho, H. K. Choi, J. Y. Lee, and J. W. Choi, "Application of gold nanoparticle to plasmonic biosensors," *Int. J. Mol. Sci.*, vol. 19, no. 7, 2018, doi: 10.3390/ijms19072021.
- [13] F. S. Halim *et al.*, "MicroRNA of N-region from SARS-CoV-2: Potential sensing components for biosensor development," *Biotechnol. Appl. Biochem.*, no. June, pp. 1–16, 2021, doi: 10.1002/bab.2239.
- [14] S. Cerra *et al.*, "Insights about the interaction of methotrexate loaded hydrophilic gold nanoparticles: Spectroscopic, morphological and structural characterizations," *Mater. Sci. Eng. C*, vol. 117, no. June, p. 111337, 2020, doi: 10.1016/j.msec.2020.111337.
- [15] Y. T. Yeh *et al.*, "A rapid and label-free platform for virus capture and identification from clinical samples," *Proc. Natl. Acad. Sci. U. S. A.*, vol. 117, no. 2, pp. 895–901, 2020, doi: 10.1073/pnas.1910113117.
- [16] P. Mahmoodi *et al.*, "Early-stage cervical cancer diagnosis based on an ultra-sensitive electrochemical DNA nanobiosensor for HPV-18 detection in real samples," *J.*

- Nanobiotechnology*, vol. 18, no. 1, pp. 1–12, 2020, doi: 10.1186/s12951-020-0577-9.
- [17] F. N. Jaapar, U. Hashim, A. R. Ruslinda, and M. N. A. Uda, “Designing DNA probe from HPV 18 and 58 in the E6 region for sensing element in the development of genosensor-based gold nanoparticles,” no. September, pp. 1–18, 2021, doi: 10.1002/bab.2260.
- [18] Y. Fu, R. Yuan, L. Xu, Y. Chai, X. Zhong, and D. Tang, “Indicator free DNA hybridization detection via EIS based on self-assembled gold nanoparticles and bilayer two-dimensional 3-mercaptopropyltrimethoxysilane onto a gold substrate,” *Biochem. Eng. J.*, vol. 23, no. 1, pp. 37–44, 2005, doi: 10.1016/j.bej.2004.10.008.
- [19] F. Colas and D. Barchiesi, “Surface modification of metal oxide films by gold nanoparticles,” doi: 10.1088/1742-6596/1319/1/012005.
- [20] J. Liu *et al.*, “An effective hydroxylation route for a highly sensitive glucose sensor using APTES/GOx functionalized AlGa_N/Ga_N high electron mobility transistor,” *RSC Adv.*, vol. 10, no. 19, pp. 11393–11399, 2020, doi: 10.1039/c9ra09446f.
- [21] R. Shahbazi *et al.*, “Highly selective and sensitive detection of Staphylococcus aureus with gold nanoparticle-based core-shell nano biosensor,” *Mol. Cell. Probes*, vol. 41, pp. 8–13, 2018, doi: 10.1016/j.mcp.2018.07.004.
- [22] J. Yoo, H. Jeong, S. K. Park, S. Park, and J. S. Lee, “Interdigitated Electrode Biosensor Based on Plasma-Deposited TiO₂ Nanoparticles for Detecting DNA,” 2021.
- [23] S. Ramanathan *et al.*, “Surface charge transduction enhancement on nano-silica and - Alumina integrated planar electrode for hybrid DNA determination,” vol. 265, no. March, 2021.
- [24] S. Nadzirah, N. Azizah, U. Hashim, S. C. B. Gopinath, and M. Kashif, “Titanium Dioxide Nanoparticle-Based Interdigitated Electrodes: A Novel Current to Voltage DNA Biosensor Recognizes E. coli O157:H7,” *PLoS One*, vol. 10, no. 10, p. e0139766, 2015, doi: 10.1371/journal.pone.0139766.
- [25] N. A. Parmin, U. Hashim, S. C. B. Gopinath, Z. Rejali, and A. Afzan, “A Sensitive DNA Biosensor using Screen Printed Gold Electrode Interdigitated Electrode (IDE) Pattern based for Identification of Human Papillomavirus Type 18 Variants,” vol. 1, no. 1, pp. 1–8, 2019.